Available online at www.sciencedirect.com
ScienceDirect
Remote Sensing of Environment 108 (2007) 311–326
Remote Sensing of Environment
www.elsevier.com/locate/rse

Comparison between current and future environmental satellite imagers on cloud classification using MODIS

Zhenglong Li [a,*], Jun Li [a], W. Paul Menzel [b], Timothy J. Schmit [b], Steven A. Ackerman [a]

[a] Cooperative Institute for Meteorological Satellite Studies (CIMSS/SSEC), University of Wisconsin-Madison, 1225 West Dayton Street, Madison, WI 53706 United States
[b] Center for Satellite Applications and Research, NOAA/NESDIS, 1225 West Dayton Street, Madison, WI 53706 United States

Received 15 April 2006; received in revised form 17 November 2006; accepted 18 November 2006

Abstract

Future Satellite Imagers are expected to improve current ones on environmental and meteorological applications. In this study, an automatic classification scheme using radiance measurements with a clustering method is applied in an attempt to compare the capability on cloud classification by different sensors: AVHRR/3, the current GOES-12 Imager, SEVIRI, VIIRS, and ABI. The MODIS cloud mask is used as the initial classification. The results are analyzed with the help of true color and RGB composite images as well as other information about surface and cloud types. Results indicate that the future sensors (ABI and VIIRS) provide much better overall cloud classification capabilities than their corresponding current sensors (the current GOES-12 Imager and AVHRR/3) from the two chosen demonstration cases. However, for a specific class, it is not always true that more spectral bands result in better classification. In order to optimally use the spectral information, it is necessary to determine which bands are more sensitive for a specific class. Spatial resolution and the signal-to-noise ratio (SNR) of satellite sensors can significantly affect the classification. The 2.13 μm band could be useful for thin low cloud detection and the 3.7 μm band is useful for fresh snow detection.

Keywords: MODIS; Cloud classification; Cloud detection; ABI; VIIRS

1. Introduction

Clouds play an important role in the earth–atmosphere system. In general, clouds significantly affect the heat budget by reflecting short-wave radiation (Hobbs & Deepak, 1981), and absorbing and emitting long-wave radiation (Hunt, 1982). Different types of clouds have different radiative effects on the earth–atmosphere system. The net effect is a function of the cloud optical properties and the properties of the underlying surface. For example, thin cirrus clouds over tropical waters have little impact on solar radiation (Liou, 1986). However, these clouds absorb long-wave radiation which increases the greenhouse effect.

Cloud detection and classification is one important task for meteorological satellites. Accurate and automatic cloud detection and classification is useful for many surface and atmospheric applications. Studies (Vázquez-Cuervo et al., 2004) show that cloud contamination and aerosols are the two main error sources (as large as 0.5 K) for infrared (IR) satellite retrieval of sea surface temperature (SST). Snow is difficult to be identified from low level clouds because both have large reflectance in visible (VIS) bands and similar thermal properties in IR bands. In order to discriminate snow cover from clouds using IR satellite measurements, cloud-filled and cloud-contaminated pixels have to be identified (Allen et al., 1990). Classification information, such as clear, single and/or multilayer cloud, from the Moderate Resolution Imaging Spectroradiometer (MODIS) measurements within a single Atmospheric Infrared Sounder (AIRS) footprint enhance the cloud clearing of AIRS radiances (Li et al., 2004, 2005). Better understanding of the cloud classification improves the retrieval of cloud top pressure, optical depth and effective radius (Frey et al., 1999; Li et al., 2001).

The simplest and probably most commonly used approach applies a set of thresholds (both static and dynamic) of reflectance, brightness temperature (BT) and brightness temperature difference (BTD) (Ackerman et al., 1998). Spatial variances/textures are also useful (Key, 1990). These methods are being

* Corresponding author. Tel.: +1 608 265 9966; fax: +1 608 262 5974.
E-mail address: Zhenglong.Li@ssec.wisc.edu (Z. Li).

0034-4257/$ - see front matter © 2006 Elsevier Inc. All rights reserved.
doi:10.1016/j.rse.2006.11.023

widely used on different imager sensors. They may fail when two different classes have similar spectral signatures. This is why the discrimination of low clouds from snow/ice is difficult for threshold methods. These threshold methods were mainly developed during the 1980s and early 1990s.

After that time, with improved computer speeds, many researchers use statistical methods to conduct cloud classification and detection. New methods, such as neural network (Key et al., 1989), Bayesian methods (Uddstrom et al., 1999), clustering analysis or maximum likelihood (Li et al., 2003), and fuzzy logic (Baum et al., 1997), have provided impressive results for cloud detection and classification. The statistical methods are supposed to be superior to the traditional threshold methods in two aspects. The former could digest more information than the latter one. For a single class, the latter uses a couple of (usually 2 to 3) bands, which are significantly sensitive to this class; while the former could use all the available bands and thus extract more useful information. Secondly, when the overlap between two classes is significant, the statistical method could optimally separate the separable parts better than the threshold methods. However, there are some short-comings in statistical methods, which limit their performance and prevent them from being used globally. For example, the neural network approach needs training sets which are region-based and Bayesian methods need information on the distribution of the data, which is now assumed to be a normal distribution while the actual data distribution may vary regionally. In contrast, the threshold methods are not affected by location and the distribution of the data, which makes them suitable for global use. This could also explain why they are still widely used.

Operational imagers on both polar orbiting and geostationary satellites monitor changes in the environment and cloud conditions. For example, the Advanced Very High Resolution Radiometer (AVHRR/3) is a 6-band imager on National Oceanic and Atmospheric Administration (NOAA) satellites and provides global cloud observations operationally (see http://www2.ncdc.noaa.gov/docs/klm/htclustering/c3/sec3-1.htm), while the current Geostationary Operational Environmental Satellite (GOES)-12 Imager provides hemispheric cloud observations every 25 min (Schmit et al., 2001). The future advanced Visible Infrared Imager/Radiometer Suite (VIIRS) will replace AVHRR/3 on the National Polar Orbiting Environmental Satellite System (NPOESS), while the Advanced Baseline Imager (ABI) (Schmit et al., 2005) on the next generation of GOES-R series will replace the current GOES Imagers (Schmit et al., 2001) for operational applications. One important question is how these advanced imagers (VIIRS and ABI) might improve the operational products over the current imagers (AVHRR/3 and the current GOES-12 Imager). In this study, we will focus on the capabilities on cloud classification by different imager sensors.

To simulate the capabilities of various imagers (current and future) on cloud detection and classification, the clustering algorithm with MODIS data is used in the study. The same method was used for MODIS cloud classification by Li et al. (2003). Instead of demonstrating the capability of MODIS on cloud classification with the clustering algorithm, this paper is focused on comparing the capability among different imager sensors with MODIS clustering classification as a standard. Similar to the statistical methods mentioned earlier, the clustering algorithm has its own shortcoming. This method highly depends on the initialization. However, this shortcoming does not prevent it from global use in this study because the MODIS cloud mask (Ackerman et al., 1998) provides a perfect initial classification for the clustering method. As described in Li et al. (2003), there are a total of 15 classes in the MODIS cloud mask (Table 1).

Section 2 introduces the data and the different imagers. Section 3 provides a brief description of the clustering algorithm. In Section 4, the capability of MODIS for cloud/surface classification is demonstrated and two cases are used to compare the different imagers. Discussions are given in Section 5, and the summary is presented in Section 6.

2. Data

2.1. MODIS data

Three types of data are used in the MODIS cloud classification. Radiances provide the primary information for surface and cloud type classification. In some situations, variance or texture images (Coakley & Bretherton, 1982; Uddstrom & Gray, 1996) and BTD are also useful for classifying the cloud and surface types (Liu et al., 2004). Table 2 shows all the data used in the MODIS clustering classification (the third column). The ocean color bands are not included in this study. LSD stands for local standard deviation, also known as the variance or texture images, and is defined as

$$\mathrm{LSD}(i,j) = \left[\sum_{m,n=-1}^{1} (x(i+m,j+n) - \bar{x})^2 \right]^{1/2}$$

where x is the radiance, $\bar{x}$ is the mean of a 3 by 3 field-of-view (FOV) area, and i j are the pixel index of the ith line and jth column. In Li et al. (2003), LSD is calculated from a 4 by 4 FOV area for bands 1–2, a 2 by 2 FOV area for bands 3–7, and a

Table 1
Initial classes from MODIS cloud mask

Class index	Content
1	Confident clear water
2	Confident clear coastal
3	Confident clear desert or semiarid ecosystems
4	Confident clear land
5	Confident clear snow or ice
6	Shadow of cloud or other clear
7	Other confident clear
8	Cirrus detected by solar bands
9	Cirrus detected by infrared bands
10	High clouds detected by CO_2 bands
11	High clouds detected by 6.7-mm band
12	High clouds detected by 1.38-mm band
13	High clouds detected by 3.7-and 12-mm bands
14	Other clouds or possible clouds
15	Others

Table 2
Data used in MODIS and other sensors clustering classification

Data	λ*	MODIS	ABI	AVHRR/3	GOES	SEVIRI	VIIRS	Primary use
Band1	659	Y	Y	Y	Y	Y	Y	Clouds, shadow
LSD-1**		Y	Y	Y	Y	Y	Y	Cirrus, low clouds, surface
Band2	865	Y	Y	Y		Y	Y	Low clouds
LSD-2		Y	Y	Y		Y	Y	Cirrus, low clouds, surface
Band3	470	Y	Y					
LSD-3		Y						
Band4	555	Y					Y	Snow
LSD-4		Y					Y	
Band5	1240	Y					Y	Snow
LSD-5		Y					Y	Clouds, snow, surface
Band6	1640	Y	Y	Y		Y	Y	Snow, shadow
LSD-6		Y	Y	Y		Y	Y	Clouds, snow, surface
Band7	2130	Y	Y				Y	
LSD-7		Y	Y				Y	
Band17	905	Y						
Band18	936	Y						Low clouds
Band19	940	Y						Shadow
Band20	3750	Y		Y			Y	Shadow
Band22	3959	Y	Y		Y	Y		
Band23	4050	Y					Y	
Band24	4465	Y						
Band25	4515	Y						
Band26	1375	Y	Y				Y	
Band27	6715	Y	Y		Y	Y		
Band28	7325	Y	Y			Y		
Band29	8550	Y	Y			Y	Y	
Band31	11,030	Y	Y	Y	Y	Y	Y	Clouds, surface
LSD-31		Y	Y	Y	Y	Y	Y	
Band32	12,020	Y	Y	Y	Y	Y	Y	Clouds, surface
LSD-32		Y	Y	Y	Y	Y	Y	
Band33	13,335	Y	Y		Y	Y		
Band34	13,635	Y						
Band35	13,935	Y						High clouds
NDVI		Y	Y	Y		Y	Y	Vegetation
NDSI		Y					Y	Snow
BT11–12		Y	Y	Y	Y	Y	Y	
BT8.6–11		Y	Y			Y	Y	Clouds
BT11–6.7		Y	Y		Y	Y		Clouds
BT3.9–3.7		Y						
BT11–3.7		Y		Y			Y	Clouds
BT12–4		Y					Y	
BT13.7–14		Y						
BT11–3.9		Y	Y		Y	Y		
Number of parameters		24	13	6	6	11	12	

*λ is the center wavelength with unit of nm.
**LSD stands for local standard deviation. Also known as variance or texture images.

3 by 3 FOV area for bands 31–32. In this paper, a 3 by 3 FOV area is used for all bands in LSD calculations.

2.2. Other imager sensors

MODIS has 36 spectral bands with 250 m to 1000 m spatial resolutions, many more spectral bands and much higher spatial resolution than other meteorological satellite imagers. Thus, MODIS data with the clustering algorithm can be used to simulate other imager sensors to compare their spectral and spatial capabilities on cloud/surface classification. This paper is focused on spectral capabilities on cloud classification by different imager sensors. For example, to simulate AVHRR/3 cloud/surface classification capabilities, MODIS bands 1, 2, 6, 20, 31 and 32 can be used. However, not all the available bands of each sensor will be used for clustering. For those bands that MODIS does not have (i.e. ABI band 6, 2.26 μm), a close band, with the similar spectral characteristics, is used as a substitute (here MODIS 2.13 μm). If no such a substitute can be found, then the band will not be used for that sensor. Although spatial resolution has important effects on classification, we will not touch this discussion until Section 5. Therefore, the resolution is approximately 1 km for all imagers in the simulation, which is the same as for MODIS.

2.2.1. ABI

The ABI will be the imager onboard the next generation GOES-R, which is scheduled to be launched in 2014 (Gurka &

Dittberner, 2001). Compared with the current GOES Imager, ABI will have more spectral bands, higher spatial resolution, and faster imaging capability (Schmit et al., 2005). These improvements offer much wider use on qualitative and quantitative weather, oceanographic, climate, and environmental applications. How the ABI will improve the current GOES class Imager (e.g., GOES-12 Imager) on cloud classification will be investigated. Of the 16 bands on the ABI, 13 are available from MODIS to be used in the clustering classification.

2.2.2. AVHRR/3

The AVHRR/3 is a six-band imaging radiometer, onboard NOAA-15, 16, 17 and 18 since 1998, with a spatial resolution of 1.1 km (see http://www2.ncdc.noaa.gov/%20docs/klm/htclustering/c3/sec3-1.htm). Compared with the previous AVHRR, a new band at 1.6 μm is designed to discriminate snow/ice from water clouds. AVHRR has been successfully used for cloud classification for a long time (Baum et al., 1997; Key et al., 1989). A lot of different methods have been developed. And many methods developed for AVHRR are now being used for other newer sensors, like MODIS and VIIRS. In this study, the AVHRR is mainly compared with VIIRS to examine how the future polar orbiting sensor will improve the current one on cloud classification.

2.2.3. The current GOES-12 imager

The current GOES class (e.g., GOES-12) Imager has a five-band multi-spectral capability on GOES 8–13 (Menzel & Purdom, 1994) with a different band available on GOES-12 and GOES-13 (Schmit et al., 2001). Unlike sensors on the polar orbiting satellites, one big advantage of the current GOES-12 Imager is its high temporal resolution which makes it suitable for short-range meteorological applications. However, lacking of near IR (NIR) bands and having only one VIS band limit its applications. The current GOES-12 Imager is included in this study to compare with ABI to demonstrate how the future geostationary imager could improve the current one. For maximum performance, all six bands are used to represent the current GOES-12 Imager.

2.2.4. SEVIRI

The Meteosat Second Generation (MSG) is a new series of European geostationary meteorological satellites (first satellite called MET-8) developed through a cooperation programme of European Space Agency (ESA) and the European Organisation for the Exploitation of Meteorological Satellites (EUMETSAT). The main instrument on board is the Spinning Enhanced Visible and Infrared Imager (SEVIRI), a 12-band radiometer providing images of the Earth disc with cloud and surface information (Schmetz et al., 2002). SEVIRI is a more advanced instrument than the current GOES Imager and AVHRR/3, but not as advanced as ABI and VIIRS (see Table 2 for the number of parameters used in the clustering algorithm for different sensors). This sensor is included in this study in order to compare the capability on classification between SEVIRI and the current/future imagers. Among the 12 bands, 11 are available from MODIS for clustering classification.

2.2.5. VIIRS

The planned VIIRS, a 22-band multi-spectral scanning radiometer, will replace AVHRR/3 onboard the NPOESS Preparatory Project (NPP) satellite in 2009, and will fly on NPOESS satellites (Lee et al., 2006). Besides the facts of more spectral bands, higher spatial resolution, better SNR and faster data acquisition, the cross track pixel expansion of VIIRS is greatly limited. Unlike MODIS and AVHRR, a unique aggregation method is used to prohibit the cross track pixel expansion. In such a way, pixels along throughout the whole swath are nearly square. This ensures the pixels at the edge of swath have useful spatial resolution. All of the improvements here offer VIIRS more chances to have better performance than AVHRR. 12 bands from MODIS are used for VIIRS cloud and surface clustering classification.

Table 2 shows the data used by each sensor for cloud/surface classification in this study.

3. Clustering classification algorithm

The clustering algorithm used in this study is the same as that in Li et al. (2003). Instead of re-describing the details of the algorithm, the main steps in the algorithm are described here:

(1) Based on MODIS cloud mask product, the mean vectors and covariance matrices of different classes are calculated.
(2) Iteration over all pixels to calculate the distances between the pixel and mean vectors of different classes.
(3) Assign the pixel to the nearest class.
(4) Update the mean vectors and covariance matrix.
(5) Go back to step 2 until convergence criteria are met.

4. Results

Two cases are shown here to compare these sensors' capabilities on cloud classification. The main reason for limiting the number of cases to two is that they are two typical challenging cases for classification. There are also some other challenging cases (i.e. dark and cold situations with near-surface thermal inversions and twilight situations). The authors are not going to make the general conclusions based on the two cases, but provide a way to compare and analyze the capabilities of different imager sensors. For both cases, two parts are provided. In the first part, interpretation of MODIS clustering classification, a detailed description of how the MODIS clustering classification is obtained is presented. In the second part, classification by different sensors, the MODIS clustering classification is used as a standard, and the clustering classifications by other sensors are compared with the MODIS clustering classification.

In this section, several different terminologies need to be clarified in advance. MODIS cloud mask is one of the operational MODIS products. It provides the cloud and surface classification information and is used as the initialization for the clustering algorithm. MODIS clustering classification is the output of the clustering algorithm using MODIS cloud mask as initialization. And it is used as the standard to compare with the classification results from other imager sensors. For example,

ABI clustering classification is the output of the clustering algorithm for ABI using MODIS cloud mask as initialization, and is compared with MODIS clustering classification (truth) for the classification performance evaluation.

4.1. Case 1: high latitude case

Cloud/surface classification in high latitude areas during the winter is challenging because of the high reflectance of surface that is often covered by snow (Allen et al., 1990). For this case we have chosen a MODIS granule at 18:55 UTC on 4 February 2004. The capability of the MODIS clustering classification is first demonstrated and then the MODIS clustering classification is used as "truth" to evaluate the capabilities of other sensors. As mentioned previously, the MODIS cloud mask is used to initialize the clustering algorithm.

4.1.1. Interpretation of MODIS clustering classification

Fig. 1(a) (b) and (d) show a Red-Green-Blue (RGB) composite image (0.65 μm, 2.13 μm and the inverse of the 11 μm), the MODIS cloud mask image, and the MODIS clustering classification image, respectively. There are 8 classes in the MODIS cloud mask image (Fig. 1(b)). It is not necessary to know what the 8 classes exactly are for two reasons. One is that some of the initial classifications are not correct (as will be shown later). The other reason is that we will redefine each class after the MODIS clustering algorithm. Actually, one may not predict what a class will be until the clustering method was performed because the final classification interpretation is highly depends on the initial classification. A cloud class will be reclassified as high clouds if it is much closer to high clouds than other class, and it will be reclassified as middle clouds if it is much closer to middle clouds than the others. Thus, the MODIS cloud mask product was used only for starting clusters and the actual labeling of the final clusters was done by interpreting the imagery thereby creating a different classification from the original MODIS cloud mask.

In this case, the MODIS clustering classification has a similar pattern to the MODIS cloud mask. With the help of the RGB composite image and the physical analysis of radiance, BTD and variance, it is possible to redefine each class.

There are 5 types of clouds in the MODIS clustering classification. The high clouds/ice clouds class is verified because it has very cold BT (average 233.39 K) in band 31 (see Table 3 for mean values for each class at the different bands). Low clouds have relatively high reflectance in VIS/NIR bands and high BT in band 31. Also $BT_{11}-BT_{12}$ has a greater value than $BT_{8.6}-BT_{11}$, which indicates low clouds (Strabala et al., 1994). Middle level clouds have spectral characteristics between high clouds and low clouds. They are brighter and colder than low clouds,

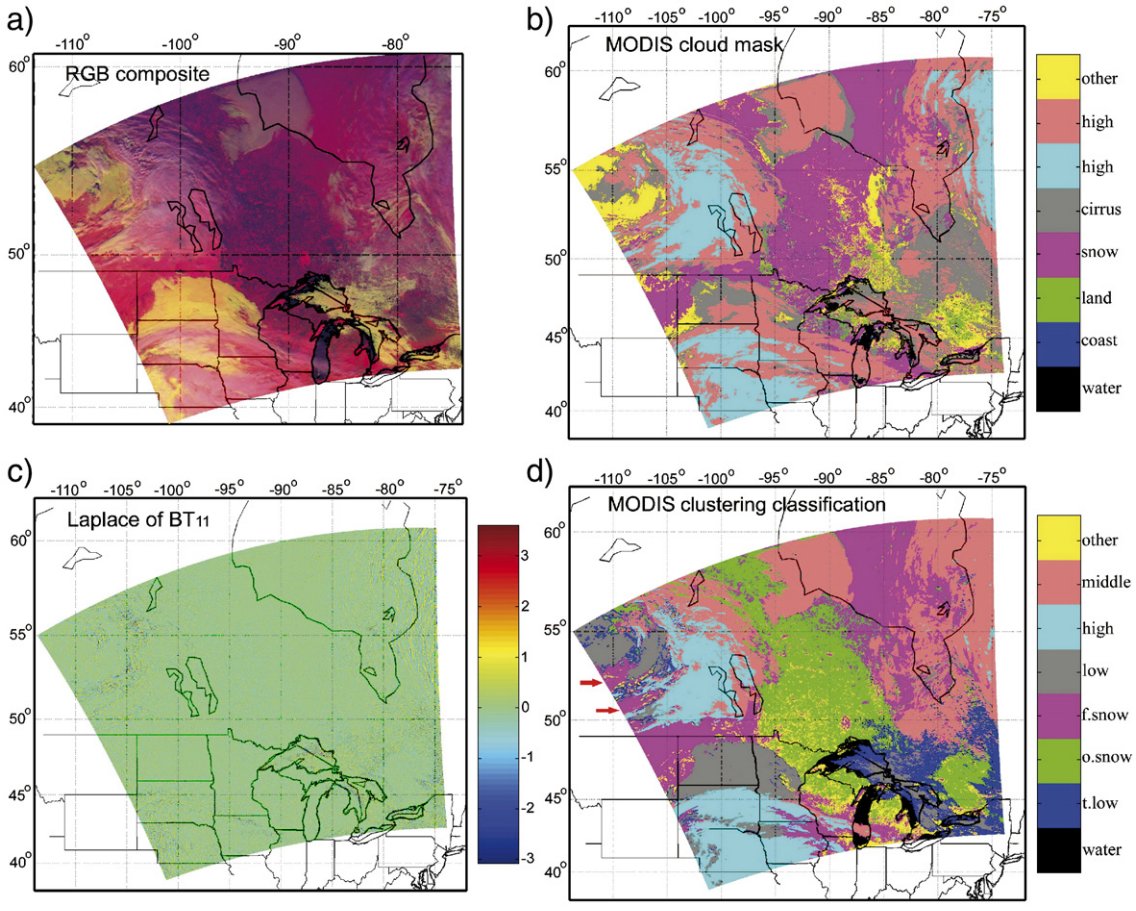

Fig. 1. (a) RGB composite image (0.65 μm, 2.13 μm and 11 μm flipped); (b) MODIS cloud mask; (c) Laplace of BT_{11}; (d) MODIS clustering classification for case 18:55 UTC February 4, 2004. The two arrows show the two regions where MODIS cloud mask fails to detect as fresh snow.

Table 3
Mean values for different classes at different bands

	λ	Water	t.low*	o.snow*	f.snow*	Low	High	Middle	Other
Band1	659	2.14	4.9	6.89	16.85	18.38	31.72	23.2	14.14
LSD-1		0.46	2.58	1.87	2.17	1.93	0.79	1.08	2.08
Band2	865	1.09	6.23	10.85	19.49	21.07	34.76	25.67	17.36
LSD-2		0.45	2.68	1.96	2.19	2.21	0.9	1.2	2.26
Band3	470	6.46	8.94	10.16	19.18	21.4	34.08	25.79	17.27
LSD-3		0.39	2.11	1.53	1.8	1.52	0.71	0.9	1.65
Band4	555	3.57	6.16	7.76	16.82	18.52	30.95	22.94	14.48
LSD-4		0.43	2.31	1.68	1.95	1.7	0.72	0.97	1.84
Band5	1240	0.51	4.35	7.78	11.17	15.53	27.27	18.93	11.99
LSD-5		0.3	1.53	1.16	1.2	1.73	0.87	0.95	1.44
Band7	2130	0.26	1.09	1.91	1.63	7.11	9.77	8.01	3.87
LSD-7		0.23	0.41	0.4	0.18	1.16	0.5	0.55	0.71
Band17	905	0.88	5.5	9.71	16.65	18.27	31.14	22.3	14.81
Band18	936	0.64	3.63	6.43	10.22	11.39	23.36	14.65	8.66
Band19	940	0.71	4.37	7.78	12.75	14.12	26.32	17.61	11.07
Band20	3750	273.06	267.34	264.31	259.02	276.84	266.19	272.24	269.65
Band22	3959	271.97	265.56	261.98	257.2	267.56	252.41	263.09	264.41
Band23	4050	269.42	263.12	259.58	256.08	261.45	247.4	257.73	260.19
Band24	4465	233.49	231.88	231.22	229.56	230.62	226.9	228.8	230.13
Band25	4515	249.86	245.92	243.89	241.1	242.12	230.08	239.55	242.47
Band26	1375	0.13	0.28	0.4	0.44	0.87	10.02	2.93	0.33
Band27	6715	242.14	240.23	239.88	238.32	238.24	225.29	233.06	238.5
Band28	7325	253.96	250.81	249.34	247.39	247.72	230.07	242.25	247.94
Band29	8550	270.81	263.71	259.62	256.04	256.45	234.93	249.47	258.62
Band31	11,030	272.11	264.48	260	256.19	257.05	233.39	249.15	259.26
LSD-31		0.28	0.65	0.31	0.36	0.68	1.1	0.72	0.41
Band32	12,020	271.49	264.17	260.03	256.05	256.71	232.66	248.6	259.13
LSD-32		0.34	0.72	0.36	0.4	0.72	1.12	0.75	0.48
Band33	13,335	254.86	250.83	248.83	246.3	245.91	228.42	241.53	247.4
Band34	13,635	244.08	241.51	240.38	239.09	238.06	225.37	234.79	238.81
Band35	13,935	236.95	235.08	234.29	233.2	232.51	223.23	229.39	232.77
NDVI		−53.09	−6.14	32.79	12.99	10.99	7.48	8.31	15.58
NDSI		132.98	113.52	92.64	122.28	72.7	78.28	76.95	93.47
BT11–12		0.63	0.31	−0.03	0.13	0.36	0.74	0.55	0.13
BT8.6–11		−1.3	−0.77	−0.37	−0.16	−0.59	1.54	0.19	−0.65
BT11–6.7		29.97	24.25	20.12	18.39	18.36	8.06	15.67	20.78
BT3.9–3.7		−1.09	−1.78	−2.33	−2.11	−9.31	−13.77	−9.84	−5.26
BT11–3.7		−0.95	−2.86	−4.32	−3.8	−20.05	−32.8	−22.93	−10.37
BT12–4		2.07	1.06	0.45	−0.16	−4.91	−14.75	−8.34	−1.05
BT13.7–14		7.12	6.43	6.09	5.87	5.61	2.06	4.64	5.89
BT11–3.9		0.15	−1.08	−1.99	−1.69	−10.73	−19.03	−13.1	−5.1

For bands 1–19 and band 26, the values are reflectance times 100. Others are brightness temperature (K).
*t.low represents thin low clouds.
*o.snow represents old snow.
*f.snow represents fresh snow.

and darker and warmer than high clouds; variances of VIS/NIR bands are larger than high clouds and less than low clouds; variances of BT_{11} are larger than low clouds and less than high clouds. This is actually a mixture of pixels overcast by spatially homogeneous and thick middle level clouds (over west Hudson Bay) and pixels partially covered by thin middle level clouds (over east Hudson Bay). Fig. 1(c) is the second order derivative (Laplace) of 11 μm. The figure is enhanced in order to better show the intermediate values. The small values in the Laplace of 11 μm over west Hudson Bay indicate thick and spatially homogeneous clouds, while the relative large values over east Hudson Bay indicate thin and inhomogeneous clouds. The fourth class of clouds is thin low clouds ("t.low" in Table 3). The class is labeled thin low clouds because of a low reflectance in the VIS/NIR bands, very high BT_{11} and it is verified by the fact that a large part of this class is over Lake Superior, which indicates that it is not snow. Also it does not show the characteristics of ice clouds. The "other" class is mixed surface type, or other clouds. Some of them are clouds (areas between Lake Michigan and Lake Huron), some of them are ice (west of Lake Superior), and some of them are snow (Green Bay). However, this class contains only a small percentage of the total pixels in the scene.

There are three classes for clear scenes. The class of water is the easiest to verify, as can be seen from the RGB composite image (Fig. 1(a)). One of the big advantages of the RGB composite image using these bands is that both fresh snow ("f.snow" in Table 3) and old snow ("o.snow" in Table 3) are

easily discriminated from low and middle level clouds. These clouds are shown in yellow while the fresh snow is light red and old snow is inhomogeneous and looks like bare surface. Fig. 2 is the snow and ice cover map from NOAA (see http://www.nohrsc.nws.gov/index.htclustering). The red rectangle shows the area of this MODIS scene. It is clear that the whole MODIS scene is covered by snow. In Fig. 1(d), the fresh snow and the old snow are distinguished by the fact that the fresh snow has a higher reflectance (0.17 of band 1) than the old snow (0.07 of band 1), and a slightly lower surface temperature (BT_{11}), with a difference of approximately 4 K (260 K for o.snow and 256.2 K for f.snow; see Table 3). This difference is mainly caused by the different reflectance in solar radiation.

Although the MODIS cloud mask has the same pattern as the MODIS clustering classification, there are improvements in the clustering classification algorithm. For example, the clustering classification discriminates fresh snow from old snow, especially two misclassified areas, located at (110 °W, 52.5°N) and (108°W, 51°N). These two areas are labeled by red arrows in Fig. 1(d). Also the classification of clouds has been improved.

However, there is one type of cloud that is not detected: thin cirrus. In this case, there are some thin cirrus clouds over Lake Michigan, but they are too thin to be classified by the clustering algorithm. Even in the BT_{11} image (not shown), it is not so evident, but it is recognizable in the $R_{1.38}$ image. The reason why this happens will be given in the next sub-section.

Another method to verify the MODIS clustering classification is to compare results with a GOES VIS/NIR/IR animation (see http://angler.larc.nasa.gov/armsgp/). Both visible (during daytime) and IR bands show the movement of clouds and the clear surface that is covered with snow.

4.1.2. Classification by different sensors

Fig. 3 shows the results of clustering classification for the different imagers. For each sensor, there are two figures to interpret the results. The left panels are the clustering classification images, while the right panels are the classification matrices C(i, j) between the results by this sensor and MODIS, which indicates the percentages of pixels of the *i*th class of MODIS clustering classification assigned to the *j*th class of the current sensor's classification. For example, $C(14, 4)=6.5\%$ (shown with an arrow in Fig. 3(b)) means that 6.5% of "other" in the MODIS clustering classification is changed to the class of "old snow" in the ABI clustering classification. Thus, larger values in diagonal elements indicate better results (more similar to the MODIS clustering classification; off-diagonal elements represent where the simulated sensors disagree with MODIS). Obviously, the percentage for each class in the MODIS clustering classification is 100%, or $\sum_{i=1}^{15} C(i,j) = 100\%$.

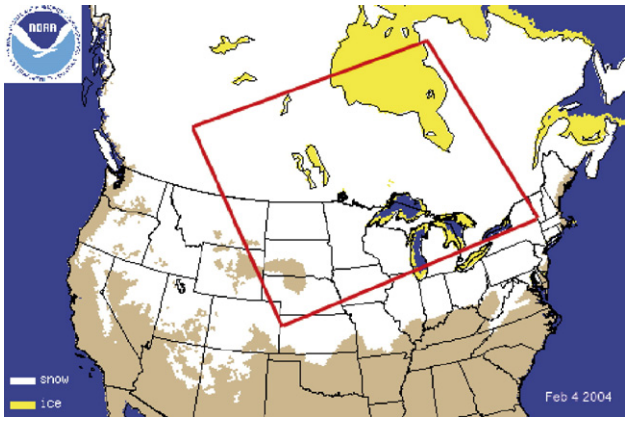

Fig. 2. Snow and ice map from NOAA. The rectangle area is the MODIS granule coverage.

Generally, all the sensors produce similar patterns of classification except the current GOES-12 Imager, which misclassifies some middle-level clouds as clear. This is because there is only one VIS/NIR band in the current GOES-12 Imager. The current GOES-12 Imager also has problems in detecting thin low clouds and old snow. However, for each class, there are some differences among the sensors.

Table 4 shows the diagonal elements $C(i, i)$ of the classification matrix for each sensor. For example, the diagonal value of low clouds for the current GOES-12 Imager is 88.6%, which means 88.6% of low clouds in the MODIS clustering classification are retained in the current GOES-12 Imager classification. The larger diagonal value corresponds the better (e.g., more MODIS-like) the classification for the sensor. Here, a diagonal value over 90% is regarded as excellent performance, 80%–90% as good performance, 70%–80% as acceptable performance and below 70% as poor performance. We define significance of likelihood (SL) as the mean of the diagonal elements of the matrix, $SL=E(C(i, i))$. This value can be used to quantitatively compare the capabilities of different sensors. The "mean" in the table is the mean value of the column.

First we will focus on the ease of detecting each class using Table 4. As expected, the class of water has the highest mean value, which means all the sensors have high capabilities to detect the open water. This is reasonable since open water is very homogeneous for almost all the bands. Low clouds are the second easiest to detect. They have a mean diagonal value of 94.4%, which indicates the classification of low clouds is very reliable for all five sensors. High clouds also have a good reliability. ABI, SEVIRI and VIIRS have diagonal values above 91.3%. Although AVHRR/3 and the current GOES-12 Imager have relatively low values (just more than 80%), the pattern is almost the same, as can be seen in Fig. 3. The main difference comes from the boundary between high clouds and middle clouds. The middle level clouds are between the high and low clouds on the vertical in the atmosphere, and thus they are usually mixed phase. This fact explains why the middle level clouds are more difficult to detect than the high and low level clouds (smaller diagonal values than the high and low clouds). In this case, the detection is even more difficult because some of the middle level clouds are thick and homogeneous clouds and some are thin and inhomogeneous clouds. For snow and thin low clouds, not all the sensors have acceptable results. ABI, SEVIRI and VIIRS are always better than average, while the GOES-12 Imager is far below average. From Table 4, the ease for detecting the classes is water > low > high > middle > thin low > fresh snow > old snow.

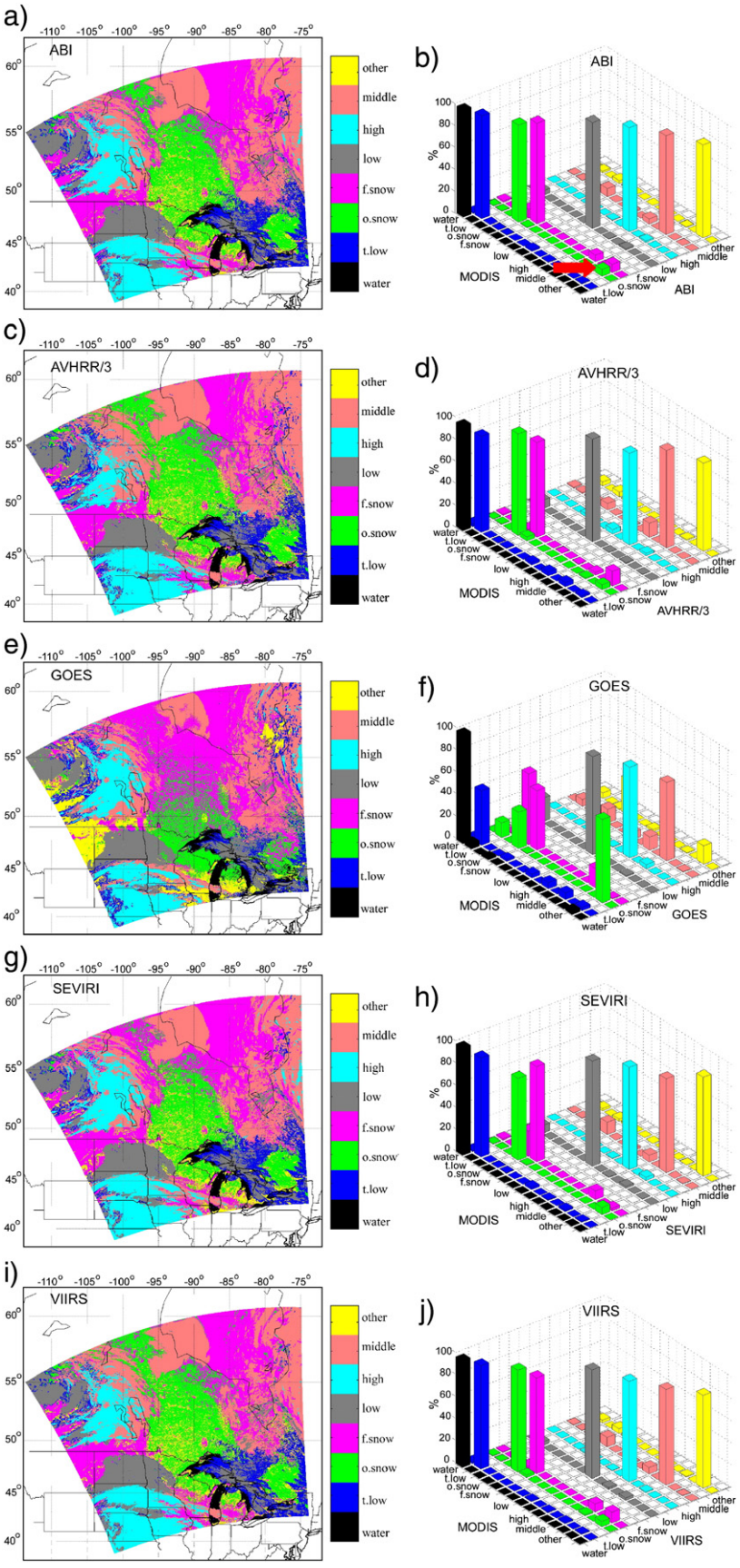

Fig. 3. Classification by different sensors (left column) and corresponding classification matrices (right column) for case 18:55 UTC February 4, 2004. From top to bottom: ABI, AVHRR/3, the current GOES-12 Imager, SEVIRI, VIIRS. Off diagonal elements in classification matrices represents where the simulated sensors disagree with MODIS.

Table 4
Diagonal values of classification matrices for different sensors, 18:55 UTC February 4, 2004

	Water	t.low	o.snow	f.snow	Low	High	Middle	Other	SL
ABI	97.4	93.7	88.6	91.7	96.3	94.8	90.2	84.6	92.2
AVHRR/3	94.8	87.1	92.4	85.9	93.3	83.2	88.6	80.0	88.2
GOES	98.5	49.0	32.9	53.4	88.6	81.9	70.9	16.8	61.5
SEVIRI	97.4	90.0	74.4	86.3	95.5	92.7	85.5	89.9	89.0
VIIRS	96.7	93.9	92.6	87.2	98.5	91.3	86.6	84.3	91.4
Mean	97.0	82.7	76.2	80.9	94.4	88.8	84.4	71.1	

Over 90% represents excellent performance. 80%–90% represents good performance. 70%–80% represents acceptable performance. Below 70% represents bad performance.

There are two methods to compare the sensors' capabilities. One compares the overall capabilities of the imagers using SL. A larger SL value indicates better overall capability. The other method compares the sensors' capabilities on different classes. This comparison is based on the diagonal values of the classification matrices.

From Fig. 3 and Table 4, for the overall performance of the imagers, it is clear that the more spectral bands, the better the results. Since future sensors have more bands than current sensors, they are expected to have better results than current ones. ABI has 13 spectral parameters used in the clustering classification and it has an excellent performance with an SL of 92.2%, the best of all. In contrast, the current GOES-12 Imager has only 6 spectral parameters, and its performance is poor with an SL of 61.5%, the worst of all. VIIRS has 12 spectral parameters while AVHRR/3 has 6. As a result, VIIRS has an SL of 91.4%, larger than the AVHRR/3 SL value of 88.2%. SEVIRI has 11 spectral parameters. It has an SL value larger than the current GOES-12 Imager and AVHRR/3 while smaller than ABI and VIIRS.

These results are reasonable because more bands provide more information, both on the surface and clouds. Table 2 (last column) shows the information of primary usage for different bands. Since the current GOES-12 Imager only has 1 VIS/NIR band, it cannot discriminate snow from clouds and fresh snow from old snow very well; it is also difficult to identify thin low clouds. A comparison between VIIRS and AVHRR/3 is interesting because AVHRR/3 has more impressive results than expected. For most classes, AVHRR/3 has only slightly smaller diagonal values than VIIRS (Table 4). In particular, for both fresh and old snow, they are almost same; 92.4% and 85.9% for AVHRR/3 while 92.6% and 87.2% for VIIRS. For middle level clouds, AVHRR/3 has a larger value than VIIRS. It seems that AVHRR/3 has almost the same information on surface and clouds that VIIRS has. However, this might not be true because AVHRR/3 cannot provide spectral information with the same radiometric precision as VIIRS. We will leave this explanation for the Discussion section.

However, these results are valid only for the sensors' overall performance. If the comparison is based on a specific class, this might not always be true. For a specific class, we cannot guarantee ABI has better classification results than the VIIRS. From Table 4, both sensors have some maximum diagonal values. This indicates each of them is better on some classes than the other. For example, ABI is better at fresh snow, high clouds, middle level clouds, while VIIRS is better at thin low clouds, old snow, low clouds. The details will depend on the differing spatial, temporal and radiometric performance, which was not taken into account in this analysis. Therefore, for a certain class/day, more bands do not necessarily yield better classification results because not all spectral information is useful for a certain class. Some bands are sensitive for snow and they are probably not sensitive for low clouds. Some are sensitive for high clouds and they are probably not sensitive for the surface. Including those insensitive bands might result in degraded classification. Take the class of water as an example, the classification using 6 bands (the current GOES-12 Imager) is better than that using 13 bands (ABI). These 6 bands are more sensitive to the class of water, while the other 7 are less sensitive. Therefore, one of the important tasks in cloud/surface classification is to determine which bands are more sensitive to a specific class.

This result also explains why the clustering method fails to classify thin cirrus clouds (in fact, almost all very thin clouds). There are only a few bands which are sensitive to cirrus, such as the 1.38 μm band and some IR bands, while other bands are not sensitive to cirrus at all. Thus, including those insensitive bands might actually decrease the relative weight of those sensitive bands since the weight for each band is fixed in the algorithm.

4.2. Case 2: desert case

Because desert has a large reflectance, it is often misclassified as low clouds by reflectance threshold tests. For the desert case we have chosen a MODIS granule at 13:00 UTC on 22 August 2004 (see Fig. 4 for the location of this granule). Focus will be on correctly identifying the desert. Fig. 4(a)–(d) shows the true color image, the surface mask, the MODIS cloud mask, and the MODIS clustering classification, respectively. The former two will be used as references to interpret MODIS clustering classification. The image of the surface type is also at 1 km resolution (Olson, 1994a,b). Since our interest is to identify the desert, we regroup the classes into only three classes (desert, land and clouds) after the clustering algorithm. The desert area includes bare desert, semi desert shrubs and hot and mild grasses and shrubs; the land area includes tropical rainforest, tropical degraded forest, rice paddy and field, savanna and woody savanna etc; and the cloudy area includes high clouds, middle level clouds, low clouds, cumulus and cirrus. In this way, the capability of discriminating desert from land is examined as well as discriminating clouds from clear (both land and desert).

4.2.1. Interpretation of MODIS clustering classification

Most of the desert area appears to be clear in the true color image (Fig. 4(a)). Those parts covered by clouds are classified successfully in the MODIS cloud mask image (Fig. 4(c)). However, many of the clear desert areas, which can be verified through the true color image, are misclassified as other clouds in the MODIS cloud mask image. For example, the southeastern part of Mauritania (black circle in Fig. 4(c)) is mostly clear

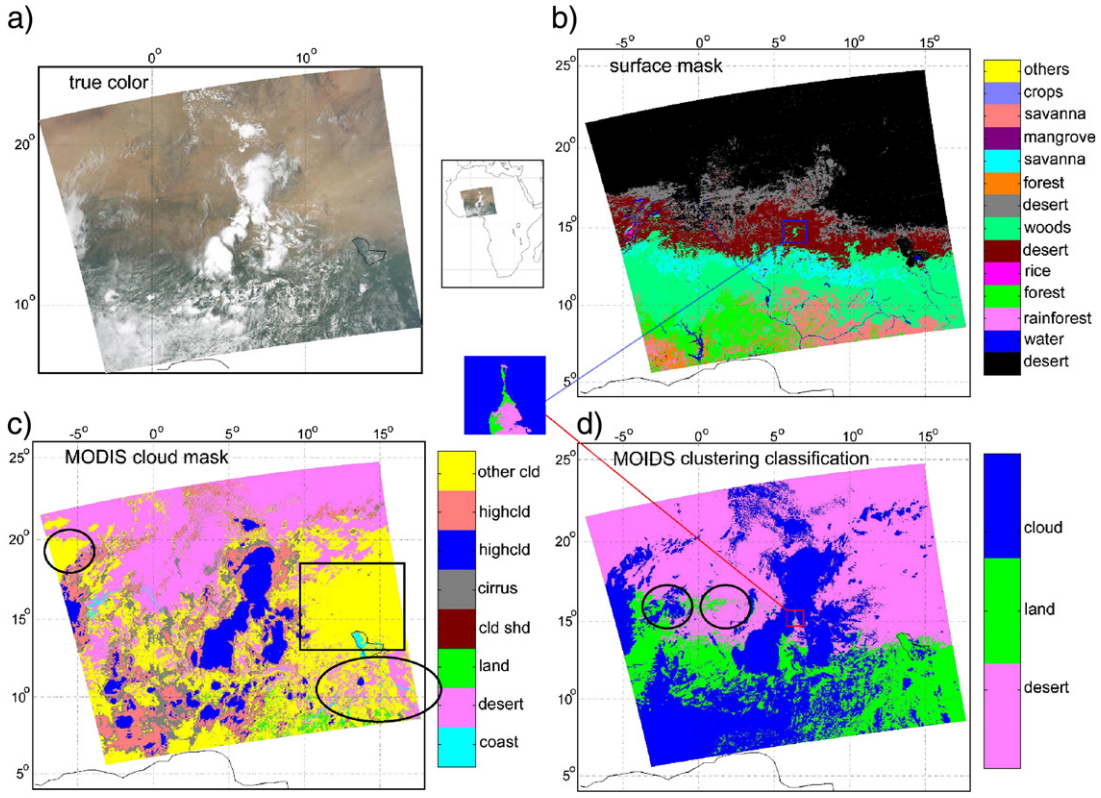

Fig. 4. (a) True color image; (b) surface mask; (c) MODIS cloud mask; (d) MODIS clustering classification for case 13:00 UTC August 22, 2004.

desert, which is classified as other clouds in the cloud mask. Also, the eastern part of Niger is clear desert (black rectangle in Fig. 4(c)), which can be verified by the true color image and is classified as other clouds. Another large misclassification is that the MODIS cloud mask misclassifies clear land as desert (black ellipse). Between 10°N and 15°N, most of the clear areas are classified as desert. However, from the surface mask image we can see these areas are mainly covered by savanna and woods, especially the northwestern part of Burkina Faso and southwestern part of Chad.

Most of the clear desert is successfully classified in the MODIS clustering classification mask (Fig. 4(d)). The line of 13°N is located approximately at the border between desert and land. North of the line is mostly desert, while south of it is mostly land. Here we treat areas of hot and mild grasses and shrubs as semi-desert. The MODIS clustering classification can even detect small green areas surrounded by desert. In the surface mask image, there is a small area of woods located at 7°E and 15°N. In the MODIS clustering classification mask, we can recognize this wood area near the clouds (see the zoomed part). The area south of these woods is classified as desert, which is consistent with the surface mask.

At the border between land and desert, there are some differences between the MODIS clustering classification mask and the surface mask because the coverage of this area has strong seasonal variation. It is desert year round, except during the rainy season when it is partly covered by green vegetation. The rainy season of Mali and Niger is from June to September. As a result, more land is detected in the clustering classification mask than the surface mask, specifically for the two relatively large areas located to the north of 15°N, which are circled in Fig. 4(d).

Most of the clouds over desert are detected very well in the MODIS clustering classification mask when compared with the true color image. Note that the cumulus in the north is successfully classified. However, over land, the detection is not very good, especially for very thin clouds. As we can see from the true color image, most land areas are covered by clouds, especially thin clouds. While in the MODIS clustering classification mask, more than half of this area is classified as clear. In fact, detection of very thin clouds, both low clouds and high clouds, is still a challenge for this algorithm. However, in this case, we mainly focus on the capability of the discrimination of desert from low clouds and other clear land.

4.2.2. Classification by different sensors

The classification results by other sensors are shown in Fig. 5 and Table 5. Again, the MODIS clustering classification mask is used as the standard. Compared with the MODIS clustering classification, all five simulated sensors have excellent performance except the current GOES-12 Imager, whose SL is only 67.8%. Furthermore, we still see the improvements of the future sensors over the current sensors. VIIRS has an SL of 95.1%, the best of all. And AVHRR/3 has an SL of 91.8%. The improvement measured by SL is 95.1%–91.8%=3.3%. Also, for each class, VIIRS performs better than AVHRR/3. For example, the classification diagonal value of desert is 97.7% for VIIRS while it is 95.1% for AVHRR/3. The improvement of ABI over the current GOES-12 Imager is even more evident.

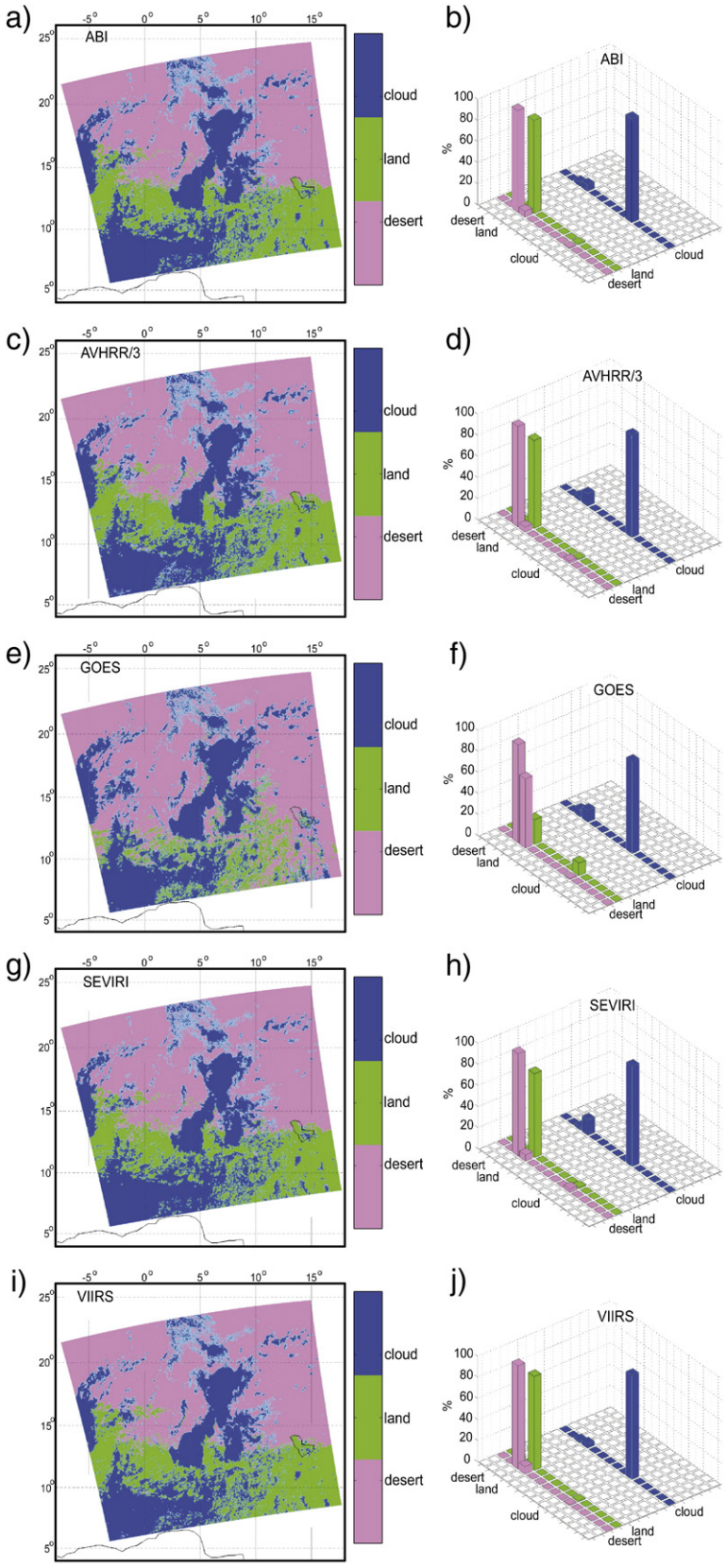

Fig. 5. Classification by different sensors (left column) and corresponding classification matrices (right column) for case 13:00 UTC August 22, 2004. From top to bottom: ABI, AVHRR/3, the current GOES-12 Imager, SEVIRI, VIIRS. Off diagonal elements in classification matrices represents where the simulated sensors disagree with MODIS.

Table 5
Diagonal values of classification matrices for different sensors, 13:00 UTC August 22, 2004

	Desert	Land	Cloud	SL
ABI	96.0	88.1	98.5	94.2
AVHRR/3	95.1	83.4	96.9	91.8
GOES	92.9	23.3	87.3	67.8
SEVIRI	97.0	79.4	95.2	90.5
VIIRS	97.7	88.8	98.7	95.1
Mean	95.7	72.6	95.3	

ABI has an excellent performance with an SL of 94.2% while the current GOES-12 Imager has a poor performance with an SL of only 67.8%. Although the current GOES-12 Imager has relatively large diagonal values for desert and cloud, the value for land is only 23.3%, which means the current GOES-12 Imager can only detect 23.3% of the land detected by the MODIS clustering classification algorithm in this particular case. This makes the results of detecting desert meaningless. Although the current GOES-12 Imager detects 92.9% of the desert areas, it also misclassifies over 60% of the land as desert (the second high pink bar in Fig. 5(f) for the current GOES-12 Imager). As for SEVIRI, since it is more advanced than the current GOES-12 Imager and AVHRR/3 and less advanced than ABI and VIIRS, results between them are expected. Indeed, SEVIRI does have better performance (SL of 90.5%) than the current GOES-12 Imager, but not as good as ABI and VIIRS.

It might not be plausible that AVHRR/3 (6 parameters) has better results than SEVIRI (11 parameters) as the results do not show what the real AVHRR/3 can achieve, as will be explained in the Discussion section. Examining the differences among the MODIS, ABI, SEVIRI and VIIRS classification results, it is found that the differences mainly come from the boundaries of different classes that are adjacent. This result is reasonable because it is hard to find an exact border (edge) to discriminate the desert from other land, and clouds from clear land.

5. Discussion

All five sensors have good capabilities on cloud/surface classification except the current GOES-12 Imager in the simulation study using MODIS data. However, in reality the current sensors (AVHRR/3, the current GOES-12 Imager and SEVIRI) might not be able to achieve such good results. There are two main reasons to constraining the performance of the current sensors.

First, the spatial resolution is not as high as with MODIS. For example, the spatial resolution is 4–8 km for the current GOES-12 Imager and approximately 3 km for SEVIRI. When the resolution is coarser, some information about the spatial variation is also smoothed out. Fig. 6(a) shows the SEVIRI clustering classification at its original spatial resolution (3 km), and Fig. 6(b) shows the classification matrix compared to MODIS. The biggest problem here is the failure to detect the middle level clouds over the west side of Hudson Bay (rectangle in Fig. 6(a)). The SL here is only 74.5% (acceptable performance), and 41.0% of middle level clouds are misclassified as fresh snow (see the pink bar labeled by an arrow in Fig. 6(b)). Besides, as the resolution decrease to 3 km, the classification diagonal values of classes of thin low clouds, old snow, fresh snow, and middle clouds are reduced by around 30%. This is consistent with what has been pointed out in the previous section; the four classes are relatively difficult to detect, therefore, they are more sensitive to the spatial resolution of the data.

The spatial resolution has different effects on the classification from sensors onboard the geostationary and polar orbiting satellites. For sensors onboard the polar orbiting satellites, the spatial resolution may affect the classification in the way discussed above. For sensors onboard the geostationary satellites, they do not have the similar viewing angle as polar orbiting satellite sensors do. Take SEVIRI as an example. Due to the high latitude in Case 1, the local zenith angle for a SEVIRI pixel could be very large, which makes the spatial resolution even coarser (worse classification as a result). Case 2 is very close to equator. And the local zenith angle could be small. Thus the

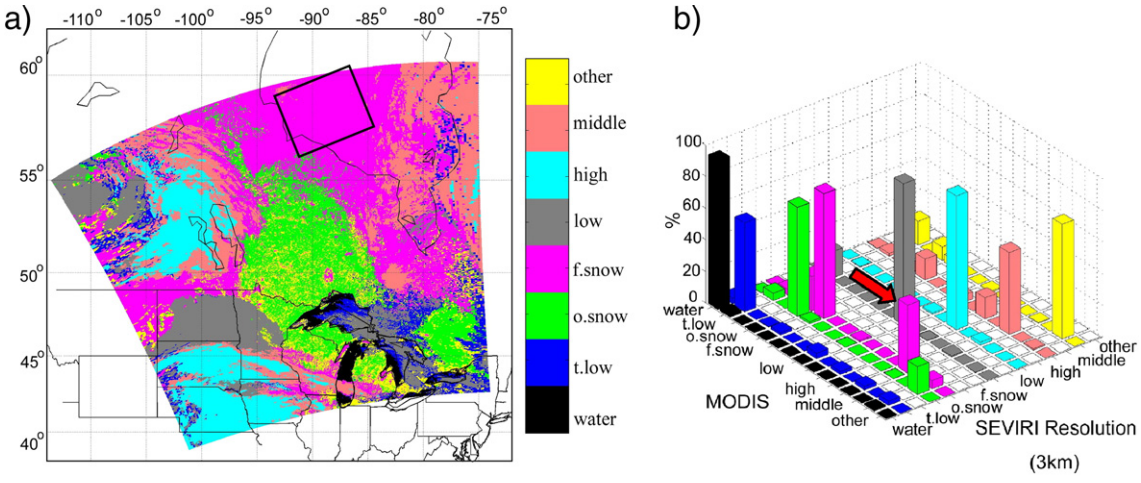

Fig. 6. Classification by SEVIRI at SEVIRI resolution (left) and corresponding classification matrix (right). The pink bar labeled shows the percentage of middle clouds which is misclassified as fresh snow in SEVIRI classification. The classification matrix is compared to MODIS clustering classification.

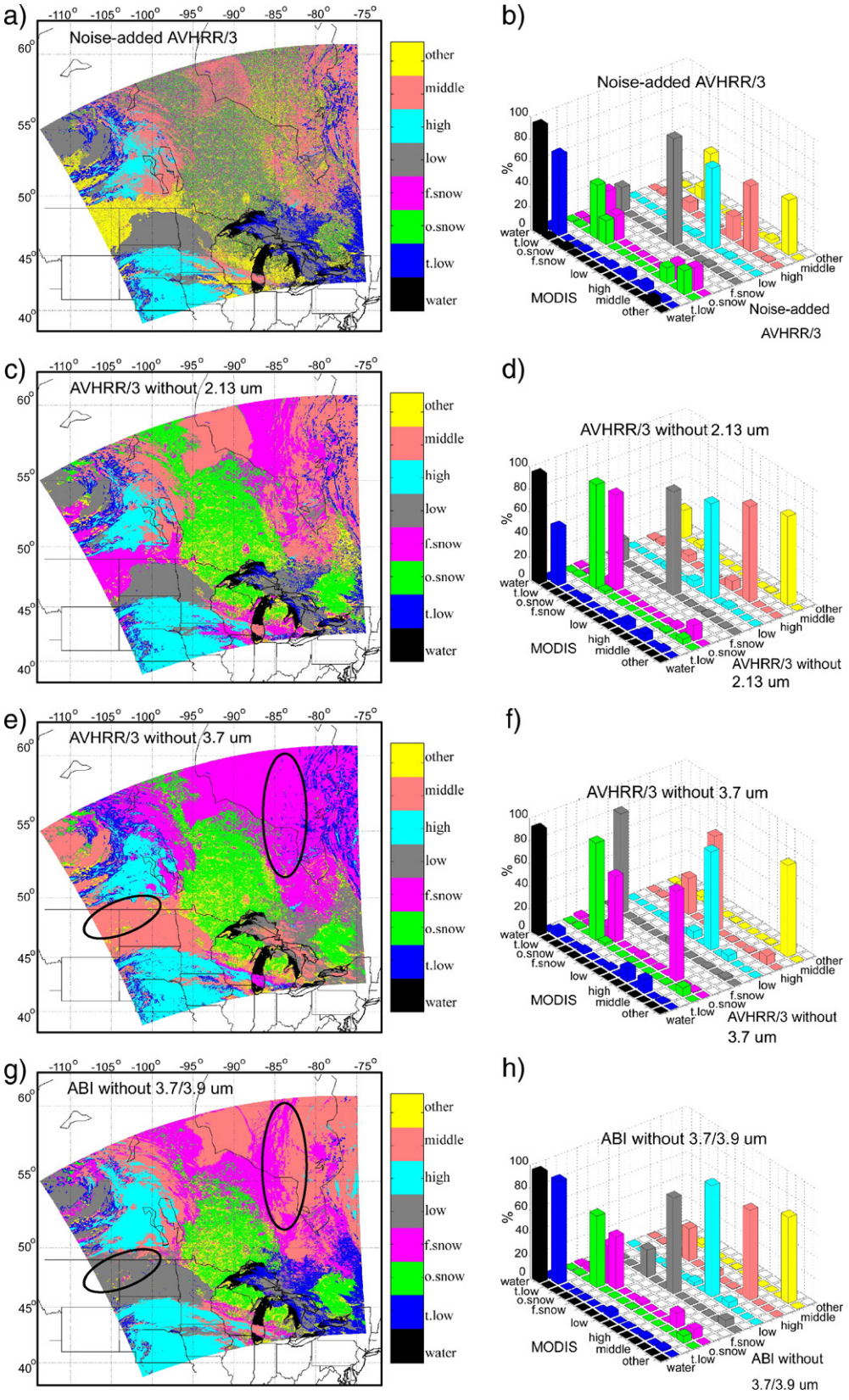

Fig. 7. Classification by (a) noise-added AVHRR/3; (c) AVHRR/3 without 2.13 μm band; (e) AVHRR/3 without 3.7 μm band; (g) ABI without 3.7/3.9 μm. The right panels are the corresponding classification matrices. Off diagonal elements in classification matrices represents where the simulated sensors disagree with MODIS.

Table 6
Classification matrix for noise-added AVHRR/3, 18:55 UTC February 4, 2004

	Water	t.low	o.snow	f.snow	Low	High	Middle	Other
Water	*95.4*	2.7	0.8	0.4	0	0.0	0.0	0.6
t.low	1.6	*71.5*	1.4	1.2	21.6	0.0	1.9	0.8
o.snow	#2.6	0.2	*47.6*	*39.1*	0.0	0.0	0.2	*10.4*
f.snow	1.0	1.2	*20.9*	*22.4*	0.0	0.2	*9.1*	*45.1*
Low	0.0	2.5	0.1	0.1	*94.4*	1.9	0.8	0.2
High	0.0	6.5	0.0	0.0	0.7	71.2	21.5	0.1
Middle	0.2	*6.4*	*14.0*	*14.6*	1.5	1.5	*58.3*	3.7
Other	6.4	2.2	21.2	20.3	0.3	0.0	1.1	48.5

The column is the MODIS classification, and the row is the noise-added AVHRR/3.
#2.6 means 2.6% of MODIS classified "water" is classified as "o.snow" by noise-added AVHRR/3. Compare with Fig. 7(b).

spatial resolution is not significantly different from the nadir for SEVIRI. Thus, for sensors onboard geostationary satellites, the classification depends on the location of selected scene. However, there is one class of exception. For thin cirrus clouds over middle or high latitude regions, if the FOV is fully filled, the optical depth is actually increased by the larger view angle from the geostationary satellite, which makes them easier to detect.

The second reason for reduced performance is that measurements by MODIS have a higher radiometric precision than the current sensors. Although AVHRR/3 has a similar resolution (1.1 km) to MODIS (1 km), the SNR is much smaller than for MODIS. Fig. 7(a) shows the noise-added clustering classification image by AVHRR/3. Noise here is normally distributed with a mean of 0 and standard deviation 1/9, 1/9, 1/20, 0.12, 0.12, 0.12 for the AVHRR/3 6 bands. The first three are exactly the reciprocal of the SNR and the latter three are the noise equivalent difference of temperature at 300 K. Fig. 7(b) shows the corresponding classification matrix comparing MODIS. For better understanding, Table 6 shows the same results. The noise has the greatest impact on fresh snow, old snow and middle clouds. The clustering classification results for these three classes are very poor. For fresh snow, only 22.4% are retained as fresh snow, while 20.9% are classified as old snow, 9.1% as middle clouds, and 45.1% as other cloud. For old snow, 47.6% are retained, whereas 39.1% are classified as fresh snow and 10.4% as other clouds. For middle clouds, 58.3% are retained, while 6.4% are classified as thin low clouds, 14.0% as old snow and 14.6% as fresh snow. For comparison, 95.4% of water and 94.4% of low clouds are retained. The analysis above shows that, for those classes that are easy to detect, such as water and low clouds, the noise does not affect them too much. But for middle level clouds, fresh snow and old snow, the effects/degradations are evident.

These results also explain why the AVHRR/3 cannot give results as good as shown in the previous section. As the precision of data decreases, the classification gets worse. Also, in practice, band 3A (band 6 of MODIS, 1.64 μm) and 3B (band 20 of MODIS, 3.7 μm) are not available simultaneously. Band 3A is on during the daytime for the purpose of snow and ice detection, while band 3B is on during the nighttime for the purpose of cloud mapping and surface temperature. It is also necessary to point out that, since 15 of the 20 detectors on Aqua MODIS band 6 are either nonfunctional or noisy, band 7 (2.13 μm) is used as a substitute of band 6. Fig. 7(c) shows the AVHRR/3 clustering classification without the 2.13 μm band, and Fig. 7(d) is the corresponding classification matrix compared to MODIS. Although it seems that the 2.13 μm band does not affect the classification very much (good performance with an SL of 82.9%), the class of thin low clouds is affected significantly. The classification diagonal value for thin low clouds is only 51.2% (poor performance) while it is 87.1% (good performance) if all 6 bands are used (Table 4). This indicates that the 2.13 μm band is probably useful for detecting thin low clouds in addition to snow and ice. Fig. 7(e) is the AVHRR/3 clustering classification without the 3.7 μm band and (f) is the corresponding classification matrix. When turning the 3.7 μm band off, the most significant problem is that it fails to discriminate fresh snow from low clouds and middle level clouds (see circled area in Fig. 7(e)). For ABI, the same situation happens when turning off the 3.7/3.9 μm band(s) (Fig. 7(g) and (h)). Note here the classification fails to assign each class. In fact, in Fig. 7(e), the class of middle level clouds should be low clouds and the class of fresh snow should be middle level clouds.

Two reasons could explain why the 2.13 μm does not work as well as 3.7 μm on snow coverage. The first reason is that 2.13 μm is not designed for snow detection as 1.64 μm. Although the 2.13 μm has been used for snow products instead

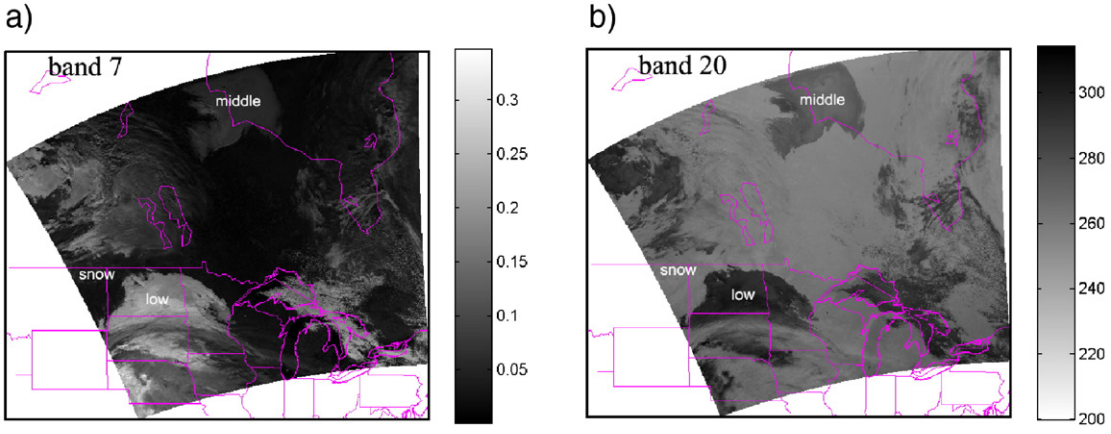

Fig. 8. (a) reflectance of band 2.13 μm; (b) brightness temperature of 3.7 μm.

of 1.64 μm (Hall et al., 2002; Salomonson & Appel, 2006), Salomonson and Appel also stated that the MODIS snow product from Aqua is not as good as from Terra. The other reason is that the contrast between snow and low/middle level clouds is not as significant on 2.13 μm imagery as on 3.7 μm imagery in this case. On Fig. 8(a), the snow area has a low reflectance while the low level clouds have high reflectance and middle level clouds have relative high reflectance. However, this contrast between snow and low/middle level clouds is more significant on 3.7 μm imagery. The snow has very low BT on Fig. 8(b), while clouds have very large BT (this band has been used for snow detection for AVHRR, see Allen et al., 1990) Thus, when turning off band 7, the detection of snow is not affected too much. But if turning off band 20, the detection of snow failed. We show 2.13 μm imagery in unit of reflectance and 3.7 μm imagery in unit of BT because these are the units used in the clustering algorithm.

Not included in this study, however, there are also other possible aspects that could affect the performance of the sensors. For example, as mentioned before, the viewing angle of satellite could change the spatial resolution, which affects the classification. The spectral response function (SRF) could affect the classification too. The normalized difference vegetation index (NDVI) and spectral reflectance are sensitive to the sensor's SRF. Trishchenko's (2002) studies show that the reflectance and NDVI measured by MODIS bands 1 and 2 could have differences as large as 30 to 40% relative to AVHRR.

6. Summary

A clustering classification algorithm, which uses the MODIS cloud mask as the initial condition, was used to compare the capabilities of different sensors on surface/cloud type detection and classification. The MODIS VIS/NIR/IR 1 km resolution spectral information and some spatial information (variance), as well as radiance differences, are used in the classification. The MODIS clustering classification is used as the reference. The study using limited cases demonstrate that:

- In general, future sensors have better overall capability on cloud/surface classification than the current ones. The main reason for this is that future sensors have more spectral bands. Both ABI (13 parameters) and VIIRS (12 parameters) show excellent performance compared to MODIS. SEVIRI (11 parameters) shows better performance than the adequate AVHRR/3 (6 parameters). While the current GOES-12 Imager (6 parameters) classification is not as good as other image sensors.
- For a specific class, it is not always true that more spectral bands result in better classification. Some bands are more sensitive than others for a specific class. Using those more sensitive bands can achieve better performance. Thus, it is important to determine which bands are more sensitive than others. This will be one topic of future work.
- Spatial resolution and SNR also impact classification. As spatial resolution becomes coarser, some information about classes of small size will be smoothed out, which results in a degraded classification. As SNR increases, the measured radiance has more precision, which results in better classification. Those classes (such as middle level clouds, fresh snow, and old snow) which are relatively hard to detect, are more sensitive to spatial resolution and SNR.
- The 3.7 μm band could be used for detection of snow. And the 2.13 μm band could be used for detection of low level thin clouds.

Acknowledgements

This program is supported by NOAA GOES-R program NA07EC0676 at CIMSS. The two anonymous reviewers are thanked for their contributions to the manuscript. The views, opinions, and findings contained in this report are those of the authors and should not be construed as an official National Oceanic and Atmospheric Administration or U.S. Government position, policy, or decision.

References

Allen, R. C., Jr., Durkee, P. A., & Wash, C. H. (1990). Snow/cloud discrimination with multispectral satellite measurements. *Journal of Applied Meteorology*, *29*, 994−1004.

Ackerman, S. A., Strabala, K. I., Menzel, W. P., Frey, R. A., Moeller, C. C., & Gueclusteringey, L. E. (1998). Discriminating clear sky from clouds with MODIS. *Journal of Geophysical Research*, *103*, 141−157.

Baum, B. A., Tovinkere, V., Titlow, J., & Welch, R. M. (1997). Automated cloud/surface classification of global AVHRR/3 data using a fuzzy logic approach. *Journal of Applied Meteorology*, *36*, 1519−1540.

Coakley, J. A., Jr., & Bretherton, F. P. (1982). Cloud cover from high resolution scanner data: Detecting and allowing for partially filled fields of view. *Journal of Geophysical Research*, *87*, 4917−4932.

Frey, R. A., Baum, B. A., Menzel, W. P., Ackerman, S. A., Moeller, C. C., & Spinhirne, J. D. (1999). A comparison of cloud top heights computed from airborne lidar and MAS radiance data using CO_2 slicing. *Journal of Geophysical Research*, *104*(24), 547−555.

Gurka, J. J., & Dittberner, G. J. (2001). The next generation GOES instruments: Status and potential impact. Preprint Volume. *5th symposium on integrated observing systems, Albuquerque, NM, 14–18 January.*

Hall, D. K., Riggs, G. A., Salomonson, V. V., DiGirolamo, N. E., & Bayr, K. J. (2002). MODIS snow-cover products. *Remote Sensing of Environment*, *83*, 181−194.

Hobbs, P. V. & Deepak, A. (Eds.). (1981). *Clouds: Their formation, optical properties and effects.* New York: Academic Press figure 2, 285 pp.

Hunt, G. E. (1982). On the sensitivity of a general circulation model climatology to changes in cloud structure and radiative properties. *Tellus*, *34*, 29−38.

Key, J. (1990). Cloud cover analysis with Arctic advanced very high resolution radiometer data. 2: Classification with spectral and textural measures. *Journal of Geophysical Research*, *95*(D6), 7661−7675.

Key, J., Maslanik, J. A., & Schweiger, A. J. (1989). Classification of merged AVHRR/3 and SMMR Arctic data with neural networks. *Photogrammetric Engineering and Remote Sensing*, *55*, 1331−1338.

Lee, T. F., Miller, S. D., Schueler, C., & Miller, S. (2006). NASA MODIS previews NPOESS VIIRS capabilities. *Weather and Forecasting*, *21*(4), 649−655.

Li, J., Liu, C. -Y., Huang, H. -L., Schmit, T. J., Wu, X., Menzel, W. P., & Gurka, J. J. (2005). Optimal cloud-clearing for AIRS radiances using MODIS. *IEEE Transactions on Geoscience and Remote Sensing*, *43*, 1266−1278.

Li, J., Menzel, W. P., & Schreiner, A. J. (2001). Variational retrieval of cloud parameters from GOES sounder longwave cloudy radiance measurements. *Journal of Applied Meteorology*, *40*, 312−330.

Li, J., Menzel, W. P., Sun, F., Schmit, T. J., & Gurka, J. J. (2004). AIRS subpixel cloud characterization using MODIS cloud products. *Journal of Applied Meteorology*, *43*, 1083−1094.

Li, J., Menzel, W. P., Yang, Z., Frey, R. A., & Ackerman, S. A. (2003). High-spatial-resolution surface and cloud-type classification from MODIS multi-spectral band measurements. *Journal of Applied Meteorology*, *42*, 204−226.

Liou, K. N. (1986). Influence of cirrus clouds on weather and climate processes: A global perspective. *Monthly Weather Review*, *114*, 1167−1199.

Liu, Y., Key, J. R., Frey, R. A., Ackerman, S. A., & Menzel, W. P. (2004). Nighttime polar cloud detection with MODIS. *Remote Sensing of Environment*, *92*, 181−194.

Menzel, W. P., & Purdom, J. F. W. (1994). Introducing GOES-I: The first of a new generation of Geostationary Operational Environmental Satellites. *Bulletin of the American Meteorological Society*, *75*, 757−781.

Olson, J. S. (1994). *Global ecosystem framework—definitions: USGS EROS data center internal report.* Sioux Falls, SD, 37 pp.

Olson, J. (1994). *Global ecosystem framework—translation strategy: USGS EROS data center internal report.* Sioux Falls, SD, 39 pp.

Salomonson, V. V., & Appel, I. (2006). Development of the Aqua MODIS NDSI fractional snow cover algorithm and validation results. *IEEE Transactions on Geoscience and Remote Sensing*, *44*(7), 1747−1756.

Schmetz, J., Pili, P., Tjemkes, S., Just, D., Kerkmann, J., Rota, S., & Ratier, A. (2002). An introduction to Meteosat Second Generation (MSG). *Bulletin of the American Meteorological Society*, *83*, 977−992.

Schmit, T. J., Gunshor, M. M., Menzel, W. P., Li, J., Bachmeier, S., & Gurka, J. J. (2005). Introducing the next-generation Advanced Baseline Imager (ABI) on GOES-R. *Bulletin of the American Meteorological Society*, *8*, 1079−1096.

Schmit, T. J., Prins, E. M., Schreiner, A. J., & Gurka, J. J. (2001). Introducing the GOES-M Imager. *National Weather Digest*, *25*, 28−37.

Strabala, K. I., Ackerman, S. A., & Menzel, W. P. (1994). Cloud properties inferred from 8–12 μm data. *Journal of Applied Meteorology*, *33*, 212−229.

Trishchenko, A. P., Cihlar, J., & Li, Z. Q. (2002). Effects of spectral response function on surface reflectance and NDVI measured with moderate resolution satellite sensors. *Remote Sensing of Environment*, *81*(1), 1−18.

Uddstrom, M. J., & Gray, W. R. (1996). Satellite cloud classification and rain-rate estimate using multi-spectral radiances and measures of spectral texture. *Journal of Applied Meteorology*, *35*, 839−858.

Uddstrom, M. J., Gray, W. R., Murphy, R., Oien, N. A., & Murray, T. (1999). A Bayesian cloud mask for sea surface temperature retrieval. *Journal of Atmospheric and Oceanic Technology*, *16*, 117−132.

Vázquez-Cuervo, J., Armstrong, E. M., & Harris, A. (2004). The effect of aerosols and clouds on the retrieval of infrared sea surface temperatures. *Journal of Climate*, *17*(20), 3921−3933.